Clays and Clay Minerals, Vol. 43, No. 2, 246–254, 1995.

QUANTIFICATION CURVES FOR XRD ANALYSIS OF MIXED-LAYER 14Å/10Å CLAY MINERALS

C. H. PONS,[1] C. DE LA CALLE,[2] AND J. L. MARTIN DE VIDALES[3]

[1] Université d'Orléans, CRMD Unité Mixte CNRS-Université, U.F.R. Faculté des Sciences
Rue de Chartres BP 6759, 45067 Orléans Cedex 2, France

[2] Instituto de Ciencia de Materiales, Sede D, C.S.I.C., c) Serrano 113
28006 Madrid, Spain

[3] Departamento de Quimica Agricola, Facultad de Ciencias
Universidad Autonoma de Madrid, 28049 Madrid, Spain

Abstract—Using theoretical profiles of diffracted X-ray intensity for interstratification between layers having d-spacings around 14.3 Å and 10.1 Å, a series of diagrams was derived from which the proportion of 14.3 Å layers (W_{14}) and the probability of passing from a 14.3 Å layer to a 10.1 Å layer ($P_{14/10}$) can be derived. W_{14} can be derived independently of $P_{14/10}$ using the angular distance between reflections situated at 18.2° and 25.4° 2θ (CuKα). Once W_{14} is determined, $P_{14/10}$ may be obtained using the angular width of the diffuse reflections between 27° and 34° 2θ. In this case, two different diagrams are proposed for $P_{14/10}$ determination because experimental X-ray patterns show either one or two diffuse reflections. Comparison of five experimental patterns with theoretical patterns calculated using W_{14} and $P_{14/10}$ obtained using these diagrams indicates that the method can be useful for determining W_{14} and $P_{14/10}$ in unknown samples. Moreover, the method described is independent of the Lorentz polarization factor and the layer type. The d-spacings associated with the two kinds of layers, however, should be similar (±1%) to those for which the determinative diagrams were calculated.

Key Words—Biotite, Chlorite, Interstratification, Mixed-layer quantification, Vermiculite.

INTRODUCTION

Numerous examples of randomly interstratified phyllosilicates in mineral deposits and in soil clays have been reported, but less common is the occurrence of regularly interstratified phyllosilicates or of interstratified phyllosilicates having a high tendency towards regularity (Bailey 1982). The presence of biotite in deep horizons of certain soils, of biotite/vermiculite interstratifications in the intermediate horizons, and of vermiculite in the upper horizons of soils suggests that during intensive weathering biotite transforms to vermiculite by means of an interstratified structure (Walker 1950, Jackson *et al* 1952, Stephen 1952, Brindley *et al* 1983, Newman and Brown 1987). Boettcher (1966), Rhoades and Coleman (1967), Sawhney (1969), and Sawhney and Reynolds (1985) demonstrated that the reverse transformation of vermiculite to mica also takes place through an intermediate interstratified state. More recently, Martin de Vidales *et al* (1990, 1991) showed that the Mg-vermiculite → K-vermiculite transformation occurs via interstratified structures.

The study of these transformations generally involves the analysis of X-ray diffraction patterns in order to determine, for each stage of the transformation, the statistical parameters of the interstratification. This can be accomplished either by calculating the distribution function of the distances between first-neighbor layers (MacEwan *et al* 1961, MacEwan and Ruiz-Amil 1975), or by comparing the experimental intensity with the theoretical intensity calculated from a structural model (Mering 1949, Kakinoki and Komura 1952, MacEwan 1956, 1958, Reynolds 1980, Plançon 1981, Pons *et al* 1981, 1989, de la Calle and Suquet 1988).

The aim of the work reported here is to present diagrams similar to those presented by Reynolds (1980), Srodon (1980), Tomita and Takahashi (1985, 1986), Tomita *et al* (1988) and Watanabe (1988). These diagrams permit rapid determination of the statistical parameters of interstratifications having d-spacings near 14.3 Å and 10 Å (notation: 14/10), and were derived from the theoretical X-ray diffraction intensity (de la Calle and Suquet 1988, Pons *et al* 1989). They are limited to interactions between nearest neighbors because interaction over a larger distance has not been found in interstratified Mg-vermiculite/K-vermiculite (Martin de Vidales *et al* 1990, 1991) or in chlorite interstratifications (Reynolds 1980, 1988).

METHODS

Calculation of the theoretical X-ray intensity

The theoretical profiles corresponding to different cases of 14/10 interstratification were calculated from the matrix expression developed by Plançon (1981), de la Calle and Suquet (1988), and Pons *et al* (1990):

$$I(2\theta) = Lp \cdot Spur(Re\{[F][W][I] + 2\Sigma_n((M - n)/M)[Q]^n\})$$

where Re signifies the Real part of the final matrix; Spur, the sum of the diagonal terms of the real matrix;

Copyright © 1995, The Clay Minerals Society

https://doi.org/10.1346/CCMN.1995.0430212 Published online by Cambridge University Press

Lp, the Lorentz-polarization and absorption factor; M, the number of layers per stack; n, an integer varying between 1 and M − 1; [F], the structure factor matrix; [I], the unit matrix; [W], the diagonal matrix of the proportions of the different kinds of layers, and [Q], the matrix representing the interference phenomena between adjacent layers. For a 14/10 interstratified system with two kinds of layers and nearest-neighbor interaction, [Q] takes the form

$$[Q] = \begin{vmatrix} P_{14/14}\exp(-2\pi i s d_{14}) & P_{14/10}\exp(-2\pi i s d_{14}) \\ P_{10/14}\exp(-2\pi i s d_{10}) & P_{10/10}\exp(-2\pi i s d_{10}) \end{vmatrix},$$

where d_{14} and d_{10} are the d-spacings of the 14 Å and 10 Å layers, respectively, $P_{14/10}$ is the probability of passing from a 14 Å layer to a 10 Å layer ($P_{14/14}$, $P_{14/10}$, $P_{10/10}$ are defined in the same way), and s is the modulus of the diffraction vector ($s = 2(\sin\theta)/\lambda$; $s = 1/d$).

The relationships between proportions of the different kinds of layers and probabilities are given by:

$$W_{14} + W_{10} = 1$$

$$P_{14/14} + P_{14/10} = 1$$

$$P_{10/14} + P_{10/10} = 1$$

$$W_{14} \cdot P_{14/10} = W_{10} \cdot P_{10/14}$$

The independent variables are W_{14} and $P_{14/10}$, the different values of which allow the calculation of all cases of interstratification, ranging from systems containing randomly distributed 14-Å and 10-Å layers to those having a regular interstratification of 14-Å and 10-Å layers. In the Appendix are given the intensity profiles obtained for different values of W_{14} and $P_{14/10}$. These patterns were calculated for layers corresponding to a natural Mg-vermiculite from Santa Olalla (Spain) (d = 14.35 Å) and its K-exchanged form (d = 10.1 Å). The parameter values used to calculate the structure factors are given in Table 1 (Shirozu and Bailey 1966, Bailey 1980, Newman and Brown 1987, de la Calle and Suquet 1988). The chosen number of layers per stack was M = 30 (a distribution of number of layers was not used) and the 2θ step was 0.02°. For the vermiculite from Santa-Olalla, this value of layers per stack corresponds to the experimental value obtained by comparing the experimental intensity with the theoretical intensity calculated with the formalism given above (Pons *et al* 1989). All theoretical patterns were calculated using the "CLARA$_2$" program for an IBM/PC or compatible.

Examination of the theoretical XRD patterns (Appendix) indicates that, for any given value of W_{14}, the reflections near 18 and 25° 2θ (Cu Kα) are only slightly affected by changes in $P_{14/10}$, whereas the angular region between 27 and 34° 2θ changes markedly with $P_{14/10}$, manifesting either 0, 1, or 2 maxima as $P_{14/10}$ varies. The calculated patterns are thus classified into three groups, namely, those displaying either 0, 1, or 2 maxima in the 27 to 34° region. These groups are clearly identified by the corresponding numbered zones in Figure 1, which is a plot, similar to that of Sato (1965), giving the relationship between $P_{10/14}$ and $P_{14/10}$ at different values of W_{14}, according to equations given above. In zones 1 and 2 interstratification may be either random (R0 order) or regular (R1 order). Zone 0 indicates the presence of a high proportion of 10-Å layers. Solid circles on the diagram correspond to the values of W_{14} and $P_{14/10}$ used for calculating the different theoretical patterns presented in the Appendix.

Table 1. Composition and atomic coordinates of the 14-Å and 10-Å layers of the St-Olalla vermiculite from Spain.

	14.35 Å			10.10 Å		
Phases	m	z		m	z	B
Layer						
O3	4.000	0.000				2.0
O2	2.000	0.100				2.0
Si	2.704	0.588				1.5
Al	1.296	0.588				1.5
O1	4.000	2.195				1.0
OH	2.000	2.368				2.0
Ti	0.034	3.315		Idem to		1.0
Fe^{2+}	0.054	3.315		14.35 Å phase		1.0
Fe^{3+}	0.472	3.315				1.0
Al	0.266	3.315				1.0
Mg	5.144	3.315				1.0
OH	2.000	4.262				2.0
O1	4.000	4.435				1.0
Al	1.296	6.042				1.5
Si	2.704	6.042				1.5
O2	2.000	6.530				2.0
O3	4.000	6.630				2.0
Interlayer						
H_2O	3.950	9.340	H_2O	0.000	—	3.5
Mg	0.453	10.490	K	0.906	8.365	2.0
H_2O	3.950	11.640	H_2O	0.000	—	3.5

m = Multiplicity. Z = Atomic coordinates in Å. B = Isotropic temperature factor.

Graphical determination of W_{14} and $P_{14/10}$

Determination of W_{14}. In Figure 2, values of W_{14} are plotted as a function of the angular distance $\delta(2\theta_{21}) = (2\theta_2 - 2\theta_1)$, where $2\theta_1$ and $2\theta_2$ are, respectively, the values of the angles corresponding to the maxima of the reflections near 18° and 25° 2θ. The definition of the angles $2\theta_1$ and $2\theta_2$ are given in Figure 3a. The width of the zone of values in Figure 2 is due to minor variations in $\delta(2\theta_{21})$ as a function of $P_{14/10}$ for a constant value of W_{14}. Practically, this means that for any value of $\delta(2\theta_{21})$, the true proportion of 14-Å layers will be between a minimum and a maximum value, namely, W_{14}(min) and W_{14}(max) which differ by a value of 0.04 (more or less) over the full range $0 < W_{14} < 1$ (Figure 2). The values of W_{14} (min) and W_{14} (max) are deter-

https://doi.org/10.1346/CCMN.1995.0430212 Published online by Cambridge University Press

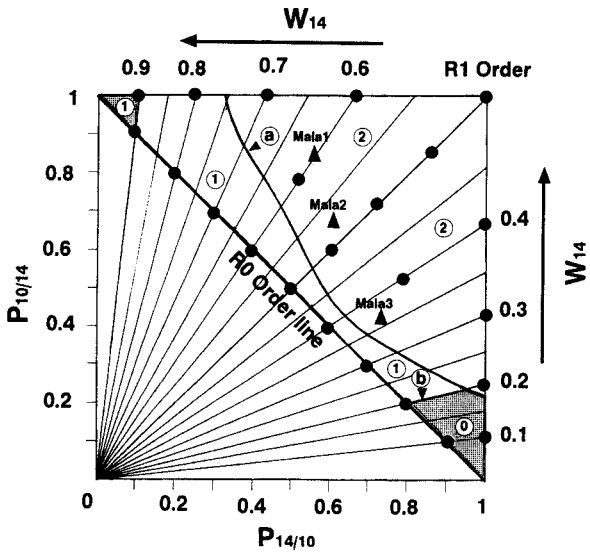


Figure 1. $P_{10/14}$ vs $P_{14/10}$ diagram for qualitative interstratification determination. ●: $P_{14/10}$ and W_{14} values used for calculating the theoretical patterns presented in the Appendix. ▲: experimental values obtained for the Malawi vermiculite samples (see Table 3). Zones corresponding to the presence of: (0) no reflection; (1) one reflection; (2) two reflections in the angular domain between 27° to 34° (CuKα). ▩: Impossible to determine $P_{14/10}$. Lines a and b indicate the limits between zones (1) and (2) and zones (0) and (1).

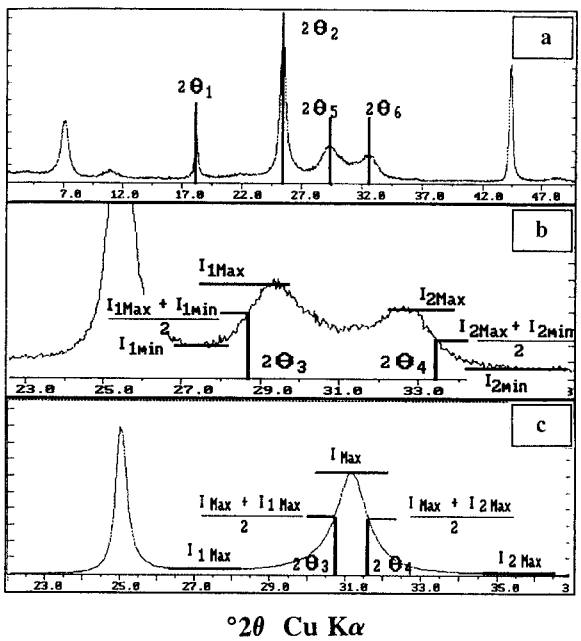


Figure 3. Definitions of the angles used in the determinative diagrams given in Figures 2, 4, and 5, in cases where, in the 2θ range 27° to 34° (CuKα), two reflections appear (a and b; experimental patterns), and one reflection appears (C; theoretical pattern).

mined from the experimentally measured angular separation $\delta(2\theta_{21})$exp, and can be used to calculate the mean value of W_{14} with a precision of ±0.02.

Determination of the probability $P_{14/10}$. Figures 4a and 4b show the values of the angular separation $\delta(2\theta_{43}) = (2\theta_4 - 2\theta_3)$ determined from the theoretical patterns and plotted as a function of $P_{14/10}$ for a given value of W_{14}. These findings correspond respectively to the cases where one or two reflections appear in the angular zone. The definitions of the angles $2\theta_4$ and $2\theta_3$ are given in Figures 3b and 3c. Using the experimental values of W_{14} obtained from Figure 2 and $\delta(2\theta_{43})$exp determined experimentally, the experimental value of $P_{14/10}$ can be taken directly from the graph (Figure 4). The relative precision is ±3% but depends on the recording accuracy of the experimental patterns (step-scan increment = 0.02° 2θ).

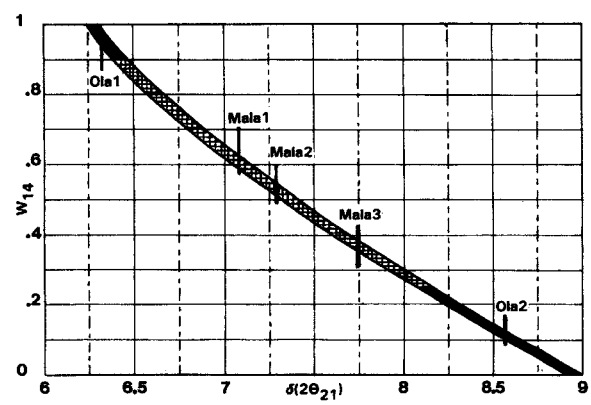


Figure 2. Diagram for quantification of W_{14} (proportion of 14 Å layers; Mg-vermiculite or chlorite) ■: zones in which $P_{14/10}$ determination is impossible. OLA 1, 2 and MALA 1, 2, 3 correspond to the samples studied (see Table 3).

Using Figure 4b, two cases are possible depending on the value of W_{14}. If $W_{14} < 0.44$ or $W_{14} > 0.7$, then the experimental value of $\delta(2\theta_{43})$exp gives a single value of $P_{14/10}$. If, on the other hand, $0.44 < W_{14} < 0.70$, then the experimental value of $\delta(2\theta_{43})$exp gives two values of $P_{14/10}$. The later case was used to construct Figure 5. This graph gives $P_{14/10}$ as a function of $\delta(2\theta_{65})$exp $= (2\theta_6 - 2\theta_5)$, where $2\theta_6$ and $2\theta_5$ are the angles corresponding respectively to the positions of the reflections situated between 27° and 34° 2θ (Figure 3a). Figure 5 should only be used for eliminating the ambiguity between the two values of $P_{14/10}$. The very considerable uncertainty in determining the value of $\delta(2\theta_{65})$, combined with the form of the curves for large values of $P_{14/10}$, gives rise to excessive uncertainty in the value of $P_{14/10}$.

The diagrams in Figures 1 and 2 and the patterns given in the Appendix reveal two groups of values of

https://doi.org/10.1346/CCMN.1995.0430212 Published online by Cambridge University Press

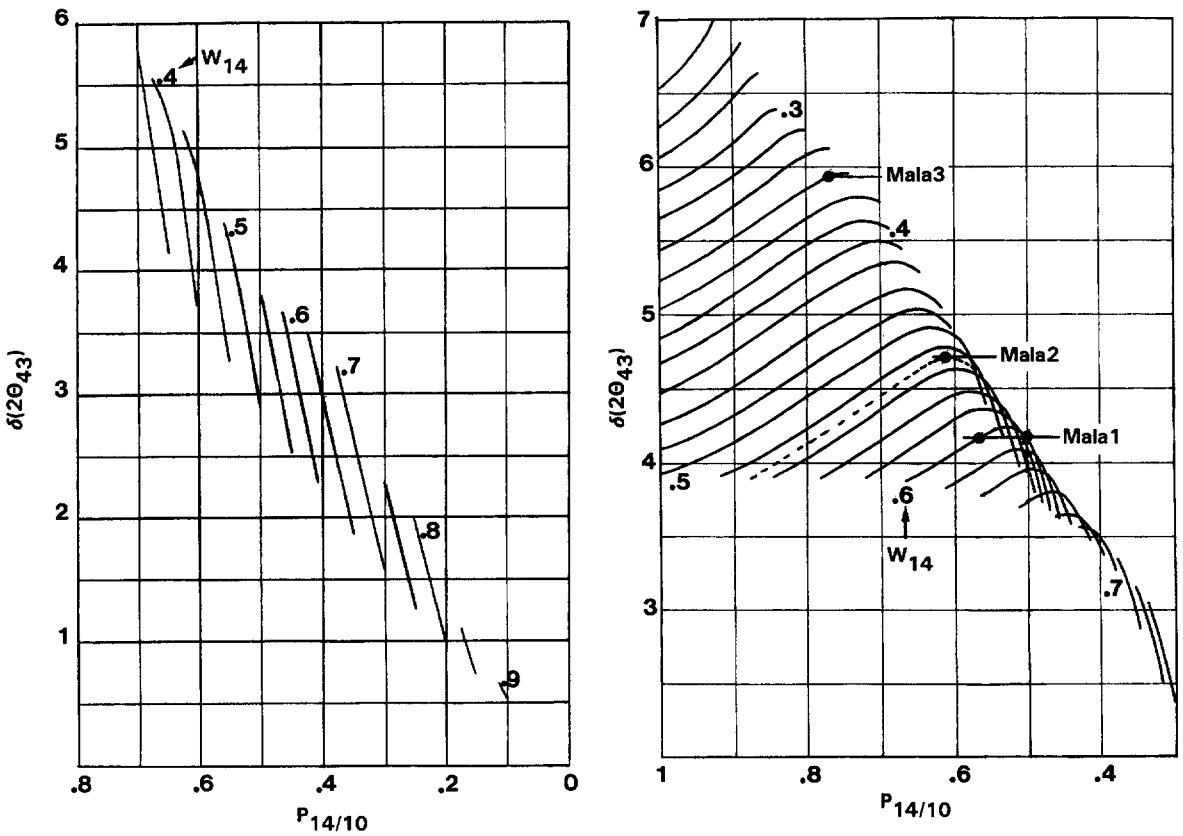


Figure 4. Relation between $\delta(2\theta_{43})$ and $P_{14/10}$ at various values of W_{14} in the 2θ range of 27–34° (CuKα), where (a) a single reflection appears, and (b) two reflections appear, $P_{14/10}$ = probability of passing from a 14-Å layer to a 10-Å layer. The dashed line in Figure 4b corresponds to $W_{14} = 0.53$. ●: experimental values for the Malawi vermiculite samples.

W_{14}, namely, $W_{14} < 0.25$ and $W_{14} > 0.9$, from which $P_{14/10}$ cannot be determined. In these two cases, the position of the reflections tends toward those belonging to pure K-vermiculite or to pure Mg-vermiculite, and the interstratification has little effect on either the breadth or position of the reflections. The interstratification does, however, affect the intensity. In order to obtain $P_{14/10}$ in these cases, comparison of the experimental curve with theoretical curves calculated from a structural model is necessary.

EXPERIMENTAL

Materials

Five interstratified K/Mg samples (Figure 6) were prepared from the Santa-Olalla vermiculite from Spain (Martin de Vidales *et al* 1991) and a Malawi vermiculite from the basement complex of southern Nyasaland (Martin de Vidales *et al* 1990). In their natural state, these two vermiculites differ in their structural 2:1 layer and interlayer compositions and in their interlayer distances (Tables 1 and 2).

Bi-ionic K-Mg interstratified vermiculites were obtained by treating cleaved sheets with mixed aqueous solutions of KCl and $MgCl_2$ having different K/Mg equivalent ratios (Table 3). The treatment consisted of combining one cleaved sheet of Mg-vermiculite (1 × 5 × 0.1 mm) with 10 ml of K-Mg solution in a sealed 20 ml teflon vessel, and heating at 160°C for 24 h. The resulting transformed sheet was washed with distilled water and dried at room temperature. The stability of the air-dried product in air was verified by X-ray diffraction (XRD) 90 days after the sample was treated.

Results

Starting from the experimental patterns and using the theoretical plots of W_{14} vs $\delta(2\theta_{12})$, the mean values of W_{14} for all the samples were determined (Table 3). The values obtained for Ola1 (95% 14 Å layers) and for Ola2 (12% 14 Å layers) corresponded to one of the cases mentioned above for which it is not possible to determine $P_{14/10}$ using the $P_{14/10}$ vs $\delta(2\theta_{43})$ diagrams, i.e., $W_{14} > 0.9$ and $W_{14} < 0.25$.

For the Mala1, Mala2, and Mala3 samples, two reflections appear in the angular zone between 27° and 34° 2θ, indicating partial R1 order (Figure 1). In Table

https://doi.org/10.1346/CCMN.1995.0430212 Published online by Cambridge University Press

Table 2. Composition and atomic coordinates of the 14-Å and 10-Å layers of the Malawi vermiculite from the basement complex of southern Nyasaland.

Phases	14.41 Å m	14.41 Å z		10.10 Å m	10.10 Å z	B
Layer						
O3	4.000	0.000				2.0
O2	2.000	0.100				2.0
Si	2.840	0.580				1.5
Al	1.040	0.580				1.5
Fe^{3+}	0.120	0.580				1.5
O1	4.000	2.160				1.0
OH	2.000	2.360		Idem to		2.0
Ti	0.102	3.300		14.41 Å phase		1.0
Fe^{3+}	0.828	3.300				1.0
Mg	5.070	3.300				1.0
OH	2.000	4.240				2.0
O1	4.000	4.440				1.0
Fe^{3+}	0.120	6.020				1.5
Al	1.040	6.020				1.5
Si	2.840	6.020				1.5
O2	2.000	6.500				2.0
O3	4.000	6.600				2.0
Interlayer						
H_2O	0.400	8.430	H_2O	0.000	—	3.5
H_2O	4.600	9.290	H_2O	0.000	—	3.5
Mg	0.453	10.480	K	0.906	8.365	2.0
H_2O	1.200	10.480	H_2O	0.000	—	3.5
H_2O	4.600	11.670	H_2O	0.000	—	3.5
H_2O	0.400	12.530	H_2O	0.000	—	3.5

m = Multiplicity. Z = Atomic coordinates in Å. B = Isotropic temperature factor.

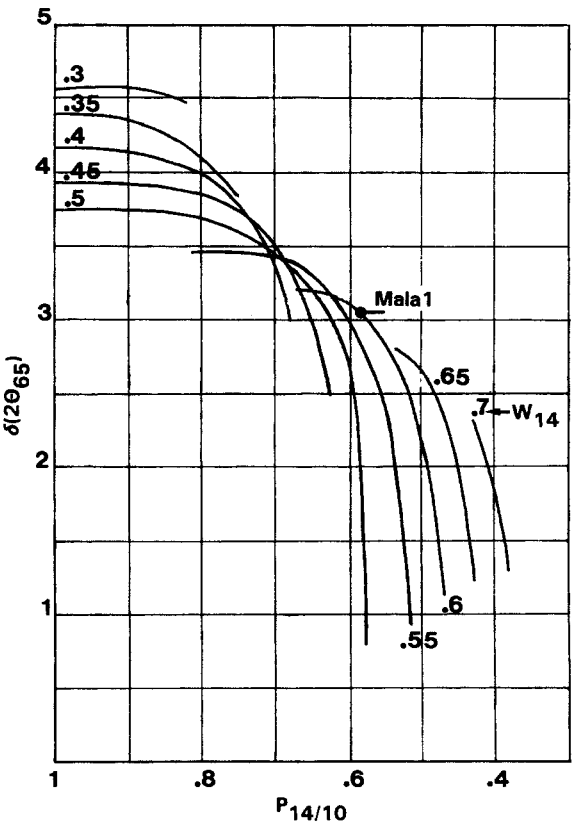


Figure 5. Relation between $P_{14/10}$ and $\delta(2\theta_{65})$ at various values of W_{14}, to be used only to remove the ambiguity in the value of $P_{14/10}$ from Figure 4b.

3 are given the values of $P_{14/10}$ determined using the diagrams presented in Figures 4b and 5.

In order to verify the accuracy of the method, the experimental patterns obtained for Mala1, Mala2, and Mala3 were compared with theoretical patterns calculated using the structure factor of Malawi vermiculite (Table 2) and the values of W_{14} and $P_{14/10}$ determined above and given Table 3. Figures 6b, 6c, and 6d show the agreement obtained between the experimental and calculated patterns. For Ola1 and Ola2 vermiculites, Figures 6a and 6e show the agreement obtained between the experimental and calculated patterns using the W_{14} values obtained above and varing only the $P_{14/10}$ parameter in the $Clara_2$ program in order to obtain the best agreement between the experimental and theoretical curves. The disagreement observed in Figure 6e between 20° and 32° 2θ is a result of diffuse background from the glass of the sample holder.

SUMMARY

The method has been shown to be useful to determine rapidly and independently the W_{14} and $P_{14/10}$ statistical parameters of interstratification. Comparisons between calculated and experimental patterns have shown the accuracy of the graphical method. In order to determine the influence of the number of layers per stack on the experimental W_{14} and $P_{14/10}$ values, a comparison was made of the values of $\delta(2\theta_{21})$ and $\delta(2\theta_{43})$ obtained by applying the proposed method to a set of theoretical curves that were calculated using different values of M. When M > 10, the results revealed that the method is independent of the number of layers per stack. This method may be applied to X-ray diffraction data obtained either with a small single crystal (Mg-vermiculite/biotite, Mg-vermiculite/K-vermiculite) or

Table 3. Values of the W_{14} and $P_{14/10}$ statistical parameters obtained for samples having different K/Mg equivalent ratios when graphical determination is (1) or is not (2) possible. The $P_{14/10}$ parameter was obtained using the $CLARA_2$ program.

Sample	Name	K/Mg	W_{14}	$P_{14/10}$ (1)	$P_{14/10}$ (2)
St-Olalla	Ola 1	1/33	0.95	—	0.05
Malawi	Mala1	1/110	0.60	0.56	
Malawi	Mala2	1/33	0.53	0.61	
Malawi	Mala3		0.36	0.76	
St-Olalla	Ola2	1/10	0.12	—	0.94

W_{14} = 14-Å layer proportion. $P_{14/10}$ = Probability of passing from a 14-Å layer to a 10-Å layer.

https://doi.org/10.1346/CCMN.1995.0430212 Published online by Cambridge University Press

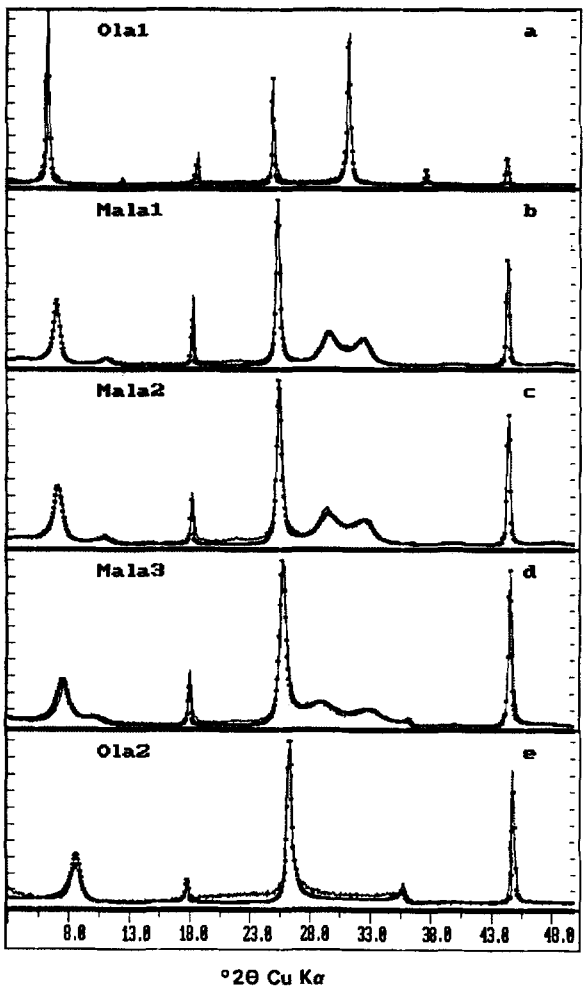


Figure 6. Comparison between experimental (——) and theoretical (■) patterns: (a) 95% 14-Å layers with partial R1 order ($P_{14/10}$ = 0.05); (b) 60% 14-Å layers with partial R1 order ($P_{14/10}$ = 0.56); (c) 53% 14-Å layers with partial R1 order ($P_{14/10}$ = 0.61); (d) 36% 14-Å layers with partial R1 order ($P_{14/10}$ = 0.76); (e) 12% 14-Å layers with partial R1 order ($P_{14/10}$ = 0.95).

with a powder sample (the normal case for most experiments). Moreover, for different samples with the same d-spacings, the composition of the 14 Å and 10 Å layers is not necessarily the same for each sample. In order to determine the influence of the Lorentz factor and the composition of the 14 Å and 10 Å layers on the W_{14} and $P_{14/10}$ values, a comparison was made of the values of W_{14} and $P_{14/10}$ obtained by applying the proposed method to a set of theoretical curves that were calculated using a Lorentz factor corresponding to either a single crystal or powder and using different types of 14 Å and 10 Å layers. The results revealed that the method is independent of the Lorentz-polarization factor and the nature of the 14 Å and 10 Å layers composing the interstratification. The only restriction is that the experimental d-spacings corresponding to the two types of layers must be similar (±1%) to the 14.35 Å and 10.1 Å d-spacings used for the determination of the diagrams giving W_{14} and $P_{14/10}$. This is important because the values of the d-spacings strongly influence the positions of the different reflections used for the determination of W_{14} and $P_{14/10}$.

ACKNOWLEDGMENT

The authors are grateful to Dr. J. W. Stucki for assistance in improving the English.

REFERENCES

Bailey, S. W. 1980. Structures of layer silicates. In *Crystal Structures of Clay Minerals and Their X-ray Identification.* G. W. Brindley and G. Brown, eds. London: Mineralogical Society, 1–123.

Bailey, S. W. 1982. Nomenclature for regular interstratification. *Clay Miner.* **17**: 243–248.

Boettcher, A. L. 1966. Vermiculite, hydrobiotite and biotite in the Rainy Creek igneous complex near Libby, Montana. *Clay Miner.* **6**: 283–296.

Brindley, G. W., and F. M. Gillery. 1956. X-ray identification of chlorite species. *Amer. Mineral.* **41**: 169–181.

Brindley, G. W., P. E. Zalba, and C. M. Bethke. 1983. Hydrobiotite, a regular 1:1 interstratification of biotite and vermiculite layers. *Amer. Mineral.* **68**: 420–425.

de la Calle, C. and H. Suquet. 1988. Vermiculite. In *Reviews in Mineralogy, Vol 19. Hydrous Phyllosilicates.* S. W. Bailey, ed. New York: Mineralogical Society of America, 455–496.

Guinier, A. 1964. *Theorie et technique de la radiocristallographie.* Chap. 13. Paris: Dunod, 490–663.

Jackson, M. L., Y. Hseung, R. B. Corey, E. J. Evans, and R. C. Vanden Heuvel. 1952. Weathering sequence of clay size minerals in soils and sediments. II Chemical weathering of layer silicate. *Soil Sci. Soc. Amer. Proc.* **16**: 3–6.

Kakinoki, J., and Y. Komura. 1952. Intensity of X-ray diffraction by one-dimensionally disordered crystals. *Jour. Phys. Soc. Japan* **7**: 30–35.

MacEwan, D. M. C. 1956. Fourier transform methods for studying scattering from lamellar systems. I. A direct method for analysing interstratified mixtures. *Koloidzeitschr.* **149**: 96–108.

MacEwan, D. M. C. 1958. Fourier transform methods for studying scattering from lamellar systems. II. The calculation of X-ray diffraction effects for various types of interstratification. *Koloidzeitschr.* **156**: 61–67.

MacEwan, D. M. C., A. Ruiz Amil, and G. Brown. 1961. Interstratified clay minerals. In *The X-Ray Identification and Crystal Structures of Clay Minerals.* G. Brown, ed. London: Mineralogical Society, 393–445.

MacEwan, D. M. C., and A. Ruiz Amil. 1975. Interstratified clay minerals. In *Soil Components. I. Inorganic Components.* G. E. Gieseking, ed. New York: Springer-Verlag, 265–334.

Martin de Vidales, J. L., E. Vila, A. Ruiz Amil, C. de la Calle, and C. H. Pons. 1990. Interstratification in Malawi vermiculite: Effect of Bi-ionic K-Mg solutions. *Clays & Clay Miner.* **38**: 513–521.

Martin de Vidales, J. L., C. de la Calle, and C. H. Pons. 1991. Interstratification K-Mg dans les vermiculites. Comportement particulier de la vermiculite de Malawi. *Clay Miner.* **26**: 571–576.

https://doi.org/10.1346/CCMN.1995.0430212 Published online by Cambridge University Press

Mering, J. 1949. Interférence des rayons X dans les systèmes a interstratification desordonnée. *Acta Crystallog.* **2**: 371–377.

Newman, A. C. D., and G. Brown. 1987. The chemical constitution of clays. In *Chemistry of Clays and Clay Minerals.* A. C. D. Newman, ed. London: Mineralogical Society, 1–128.

Plançon, A. 1981. Diffraction by layer structures containing different kinds of layers and stacking faults. *J. Applied Crystallogr.* **14**: 300–304.

Pons, C. H., F. Rousseaux, and D. Tchoubar. 1981. Utilisation du rayonnement synchrotron en diffusion aux petits angles pour l'étude du gonflement des smectites. I. Etude du système eau montmorillonite-Na en fonction de la température. *Clay Miner.* **16**: 23–42.

Pons, C. H., A. Pozzuoli, J. A. Rausell-Colom, and C. de la Calle. 1989. Mécanisme de passage de l'état hydraté à une couche à l'état zéro couche d'une vermiculite-Li de Santa Olalla. *Clay Miner.* **24**: 479–494.

Reynolds, R. C. 1980. Interstratified clay minerals. In *Crystal Structures of Clay Minerals and Their X-Ray Identification.* G. W. Brindley and G. Brown, eds. London: Mineralogical Society, 249–303.

Reynolds, R. C. 1988. Mixed layer chlorite minerals. In *Reviews in Mineralogy, Vol 19. Hydrous Phyllosilicates.* S. W. Bailey, ed. New York: Mineralogical Society of America, 601–629.

Rhoades, J. D., and N. T. Coleman. 1967. Interstratification in vermiculite and biotite produced by potassium sorption. I. Evaluation by simple X-ray diffraction pattern inspection. *Soil Sci. Soc. Amer. Proc.* **31**: 366–372.

Sato, M. 1965. Structure of interstratified (mixed-layer) minerals. *Nature* **208**: 70–80.

Sawhney, B. L. 1969. Regularity of interstratification as affected by charge density in layer silicates. *Soil Sci. Soc. Amer. Proc.* **33**: 42–46.

Sawhney, B. L., and R. C. Reynolds. 1985. Interstratified clays as fundamental particles: A discussion. *Clays & Clay Miner.* **33**: 559.

Shirozu, H., and S. W. Bailey. 1966. Crystal structure of a two-layer Mg-vermiculite. *Amer. Mineral.* **51**: 1124–1143.

Srodon, J. 1980. Precise identification of illite/smectite interstratifications by X-ray powder diffraction. *Clays & Clay Miner.* **28**: 401–411.

Stephen, I. 1952. A study of rock weathering with reference to the Malvern Hills. Part I. Weathering of biotite and granite. *J. Soil Sci.* **87**: 20–33.

Tomita, K., and H. Takahashi. 1985. Curves for the quantification of mica/smectite and chlorite/smectite interstratifications by X-ray powder diffraction. *Clays & Clay Miner.* **33**: 379–390.

Tomita, K., and H. Takahashi. 1986. Quantification curves for the X-ray diffraction analysis of mixed-layer kaolinite/smectite. *Clays & Clay Miner.* **34**: 323–329.

Tomita, K., H. Takahashi, and T. Watanabe. 1988. Quantification curves for mica/smectite interstratifications by X-ray powder diffraction. *Clays & Clay Miner.* **36**: 258–262.

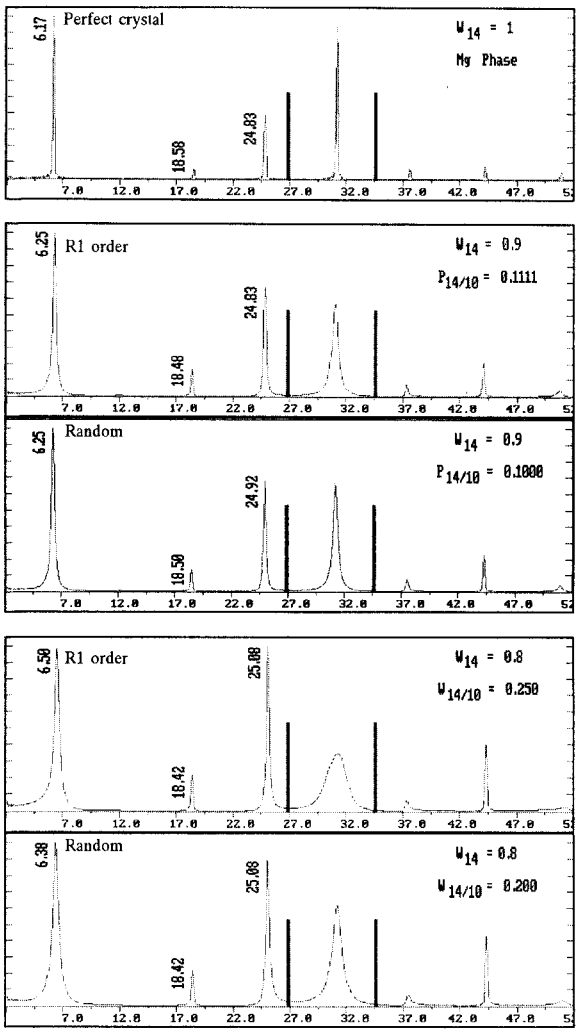
Walker, G. F. 1950. Trioctahedral minerals in the soil clays of northeast Scotland. *Mineral. Mag.* **29**: 72–84.

Watanabe, T. 1988. The structural model of illite/smectite interstratified mineral and the diagram for its identification. *Applied Clay Science* **7**: 97–114.

(Received 26 January 1993; accepted 8 August 1994; Ms. 2317)

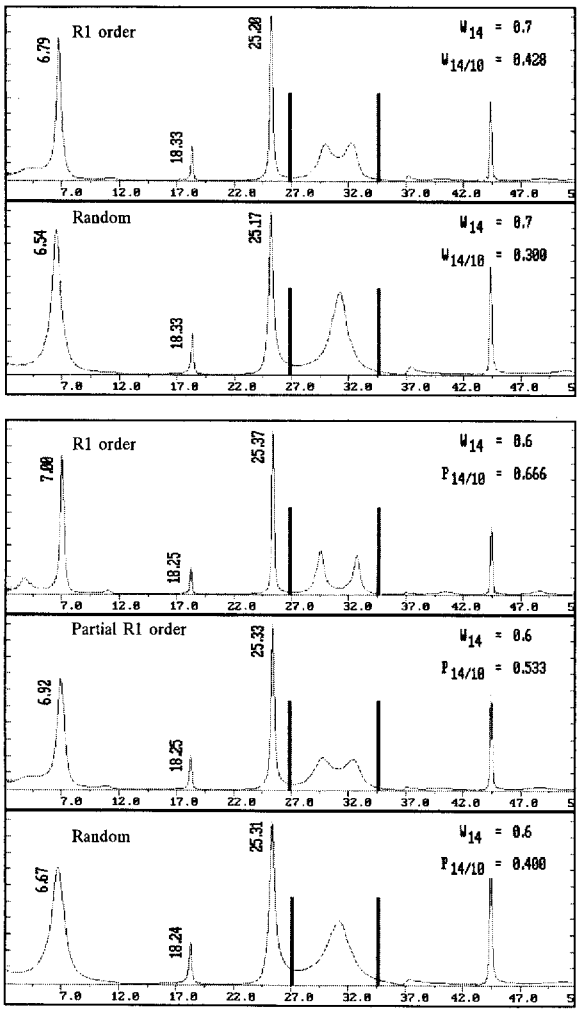
APPENDIX

Theoretical curves calculated using the program CLARA$_2$ for the determination of diagrams giving W_{14} and $P_{14/10}$ statistical parameters. W_{14} and $P_{14/10}$ values correspond to the solid circles in Figure 1. See also Figure 1 to describe the ordering implied. The vertical lines mark the angular zones sensitive to $P_{14/10}$.

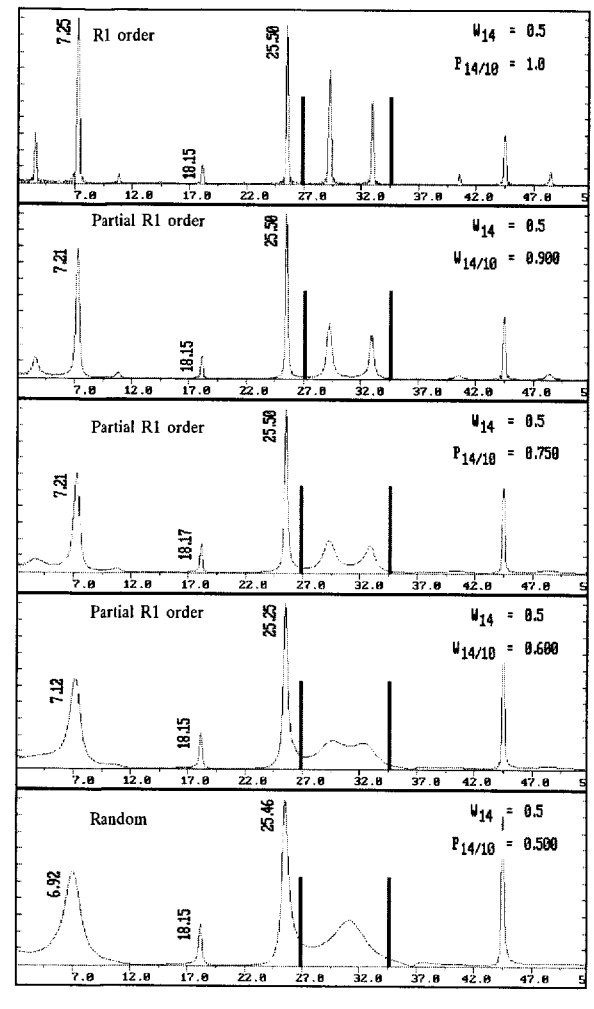


Appendix 1

https://doi.org/10.1346/CCMN.1995.0430212 Published online by Cambridge University Press

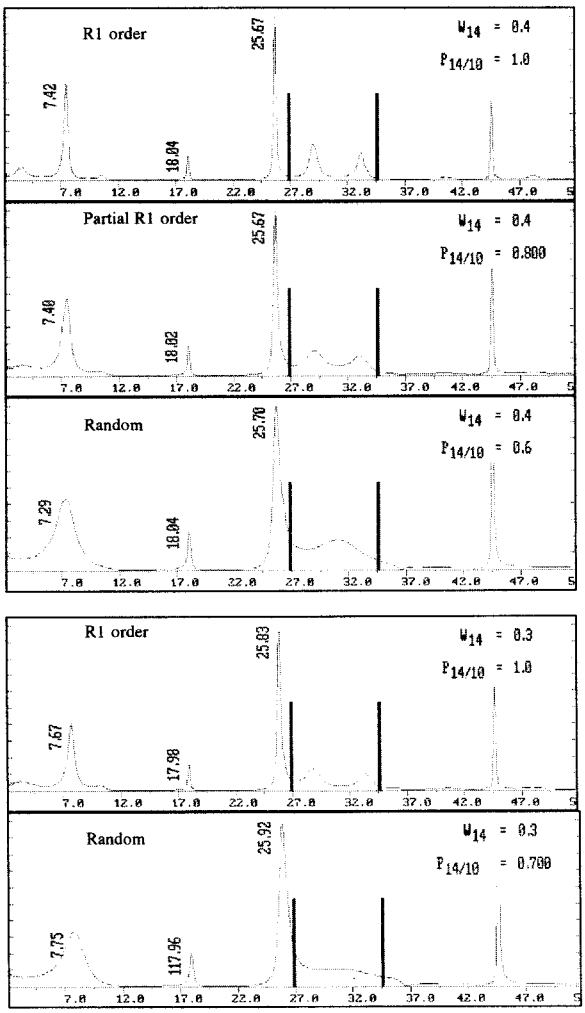


Appendix 2

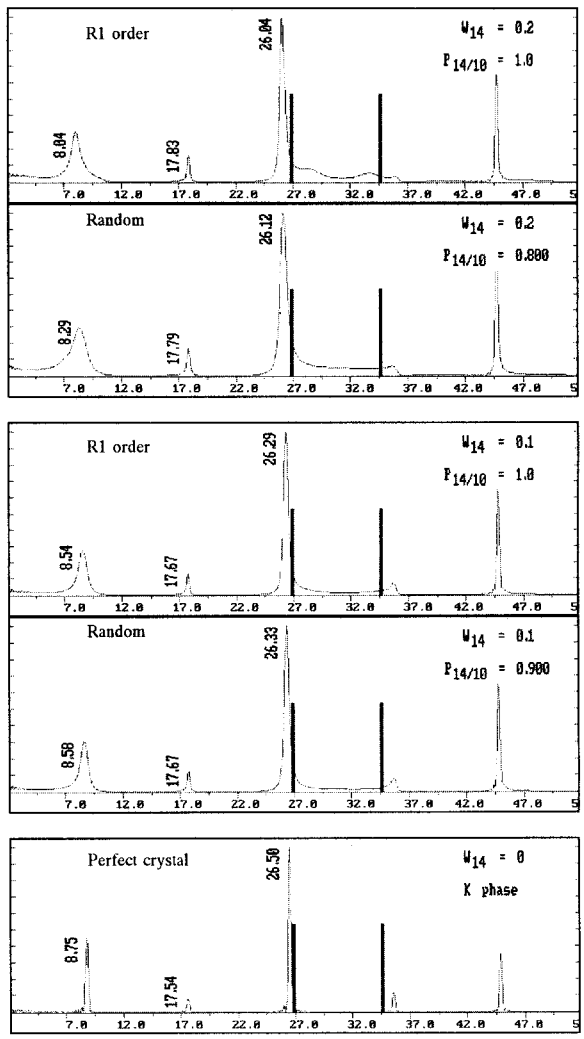


Appendix 3

https://doi.org/10.1346/CCMN.1995.0430212 Published online by Cambridge University Press



Appendix 4



Appendix 5

https://doi.org/10.1346/CCMN.1995.0430212 Published online by Cambridge University Press